

PROCEEDINGS OF SPIE

[SPIDigitalLibrary.org/conference-proceedings-of-spie](https://spiedigitallibrary.org/conference-proceedings-of-spie)

Roadside IED detection using subsurface imaging radar and rotary UAV

Yexian Qin, Jones O. Twumasi, Viet Q. Le, Yu-Jiun Ren,
C. P. Lai, et al.

Yexian Qin, Jones O. Twumasi, Viet Q. Le, Yu-Jiun Ren, C. P. Lai, Tzuyang Yu, "Roadside IED detection using subsurface imaging radar and rotary UAV," Proc. SPIE 9823, Detection and Sensing of Mines, Explosive Objects, and Obscured Targets XXI, 982317 (3 May 2016); doi: 10.1117/12.2223445

SPIE.

Event: SPIE Defense + Security, 2016, Baltimore, Maryland, United States

Roadside IED Detection Using Subsurface Imaging Radar and Rotary UAV

Yexian Qin^{*a}, Jones O. Twumasi^b, Viet Q. Le^b, Yu-Jiun Ren^{*a}, C. P. Lai, and Tzuyang Yu^b

^aCivilSensing, Rockville, MD 20850, USA;

^bDept. of Civil & Environmental Eng., Univ. of Massachusetts Lowell, One University Ave., Lowell, MA 01854, USA

ABSTRACT

Modern improvised explosive device (IED) and mine detection sensors using microwave technology are based on ground penetrating radar operated by a ground vehicle. Vehicle size, road conditions, and obstacles along the troop marching direction limit operation of such sensors. This paper presents a new conceptual design using a rotary unmanned aerial vehicle (UAV) to carry subsurface imaging radar for roadside IED detection. We have built a UAV flight simulator with the subsurface imaging radar running in a laboratory environment and tested it with non-metallic and metallic IED-like targets. From the initial lab results, we can detect the IED-like target 10-cm below road surface while carried by a UAV platform. One of the challenges is to design the radar and antenna system for a very small payload (less than 3 lb). The motion compensation algorithm is also critical to the imaging quality. In this paper, we also demonstrated the algorithm simulation and experimental imaging results with different IED target materials, sizes, and clutters.

Keywords: UAV, SAR, IED, Radar, Remote Sensing,

1. INTRODUCTION

1.1 Background

Drones are more formally known as small unmanned aerial vehicles (UAV). Essentially, a drone is a flying robot. The aircraft may be remotely controlled or can fly autonomously through software-controlled flight plans in their embedded systems working in conjunction with the GPS. UAVs have most often been associated with the military applications but they are also used for search and rescue, surveillance, traffic monitoring, weather monitoring and firefighting, among other things. More recently, the UAV has come into consideration for a number of commercial applications. Personal drones are also becoming increasingly popular, often for the drone-based photography. The most popular personal drones are rotary types drones. Rotary (multi-copter) drones are easier to operate and more accessible to either open or obstacle space than fixed-wing drones. The main drawbacks to rotary drones are slower speeds and shorter range than fixed-wing drones; even with battery extenders, most can't run more than a half-hour. To solve the flight time issues, some rotary drones can be operated through cable tethering with a generator or a portable high-volume battery. In battle field, military personnel operating a small UAV to detect IED treats is not new but mostly fixed wing UAVs are used which provide a wider area of view from a remote distance. Since those fixed wing UAVs cannot operate under a low altitude close to the ground due to its maneuver ability and minimum flight speed, it limits the probability to detect buried IEDs. To fill the detection gaps of using fixed wing UAVs, using a personal drone for IED detection can further improve IED detection performance and reduce the false alarm rate. It can secure and sweep the mission critical zone with more closely view and the detection under road subsurface. It can also give real-time update and alert team members right behind it.

In this paper, we start with the concept of operation in Section 1.2, including flight path planning, payload, and required functions. Section 2 presents the radar system, data processing, and lab testing test results. Sections 3 will discuss the modeling and simulation with different types of IED and with ground reflection analysis. The preliminary field testing results are present in Section 4. Future work and conclusion are given in Section 5.

1.2 Concept of operation

The proposed rotary UAV IED detection system (RUIED) consists of (1) a lightweight imaging radar for 3D-scanning, (2) optical cameras for the user's inspection of suspicious target from IED detection and guidance as an option in

addition to the future features of autonomous mission planning, (3) a ground control terminal, and (4) a rotary UAV which can provide a 3-lb payload and its flight time is greater than 30 minutes.

Figure 1 illustrates the operation and flight path planning for RUIED to detect roadside IEDs. RUIED will allow users to:

- i) Survey the large zone with future military activities that will happen.
- ii) Provide localized scanning around the suspicious area with visual inspection through a wireless camera.
- iii) Send multiple RUIEDs to complete the scanning with the shortest time.
- iv) Broadcast the treats from a high altitude after the IED detection.

The work concept is simple but it does take a lot of engineering efforts to make our first prototype system and the testing in both laboratory and outdoor environments.

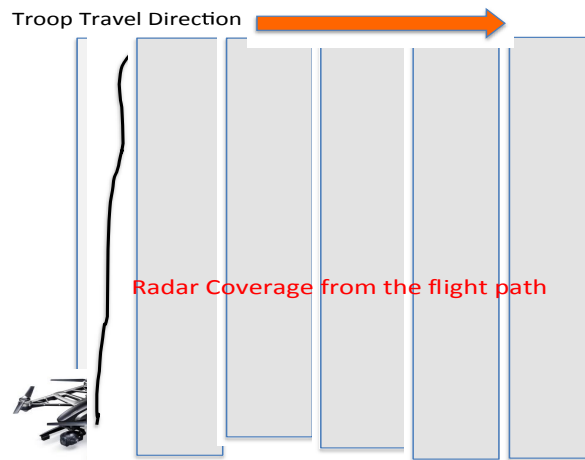


Figure 1. Operation overview of a rotary UAV IED detection system.

2. IED DETECTION USING DRONE IMAGING RADAR (DAVID LAI)

2.1 System architecture

In this work, a new RUIED is developing to detect the roadside IED by utilizing surface electromagnetic (EM) reflections collected by a compact radar system. Subsurface imaging and target detection are achieved by processing reflection measurements at different frequencies, relative elevations, inspection angles, and signal polarizations, using synthetic aperture radar (SAR) algorithms [1][2][3]. Possible frequency bands to be explored include X-band (8-12 GHz), S-band (2-4 GHz), and UHF-band (0.3-3 GHz) [4] [5]. Figure 2 shows the surface-scanning scheme of a RUIED on a road or a soil surface with/without the pavement.

The design purpose of the prototype instrument is to validate the detection of different IED types and their buried depths through the RUIED. A higher frequency band of operation is selected because of commercially available transmitters, components, and antennas for their relatively small size, and low costs. The design can be transported to other bands if desired. The system needs to be low-cost, light weight, and possess scalability. Transmission-reflection (T-R) phase coherency is not required because only non-Doppler operations are supported. However, phase and amplitude coherency within all receive channels are required. The aperture size limitation of the RUIED sensor platform confines the angular resolution to about 10° .

The important aspect of the proposed design is scalability of the transceiver system. A wideband radar transmitter is used as the basis of the transmit system. The minimum system in this design employs a high gain directional horn antenna, while the antenna gain can be changed from 15 to 22 dBi. The beam scanning relies on the RUIED moving in a designed

flight route and also the SAR imaging algorithms, such as Stripmap SAR or Spotmap SAR. Advanced beamforming can also be supported by modifying the collected imaging data in each scanning location with uniform interval.

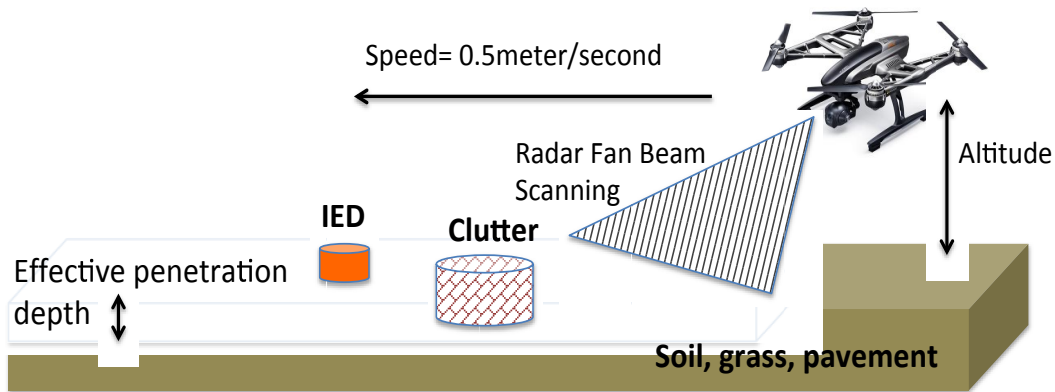


Figure 2. Inspection and monitoring schemes of the RUIED on soil, grass, or different surfaces.

2.2 Data process flow and laboratory calibration

Figure 3 shows the proposed data processing flow. Before operation, the radar system must be calibrated in-lab with small-size calibration targets. The timing cycle of the radar starts from power-up of the transceiver. Synchronization between the transmit trigger and the scan angle will ensure that the data acquisition starts when the angle is stabilized and a transmit signal has been sent. At each angle, return signals are sampled according to range gate setting and the desired surveillance range. The transmit wideband signal are sent in H-/V-polarizations and the return signals are received in H-polarized or V-polarized channels, depending on commands. This configuration enables the calculation of three variables: reflectivity, differential reflectivity and differential phase. With a pre-designed, continuous bandpass filter, the rate of image reconstruction processing can be accelerated to only a few seconds. Performance of radar signals with different polarizations (e.g., transverse electric (TE) and transverse magnetic (TM)) will be investigated and integrated to form polarimetric SAR images for the damage detection.

The advantages of the proposed distant radar sensing and imaging technique over other existing methods include: 1) large-area sensing using a flexible inspection distance; 2) effective inspection by optimal combinations of sensing mode, frequency, distance, angle, and signal polarization for different types of defect and damage; 3) data visualization by SAR operations and back-projection algorithms; 4) efficient inspection by two types of inspection (preliminary/broad and detailed). In the proposed RUIED, target detection will be conducted at two levels, raw returned signal and reconstructed image. This innovation provides with flexibility in the interpretation of results for IED detection.

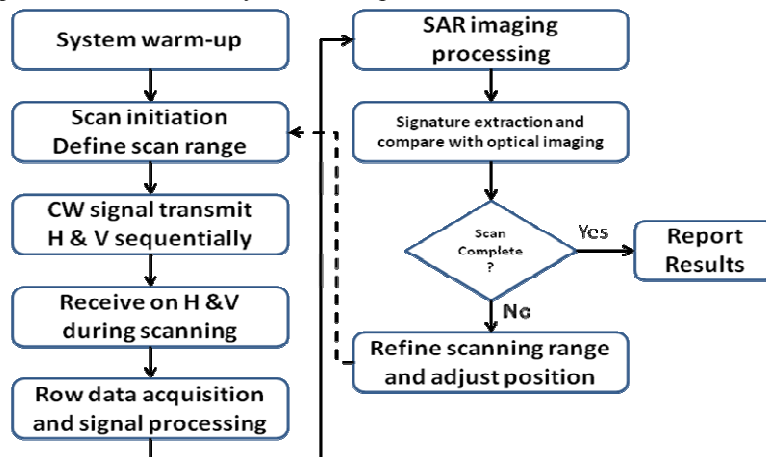


Figure 3. System data processing flow of the RUIED.

In Figure 4, the laboratory calibration of the RUIED is presented where the collected returned calibration target signals can be measured. The right size and reflection characteristics can be corrected based on the radar imaging results and the theoretical calculation. The calibration factors will be provided when the scanning angle and the antenna height are varied. Typical calibration targets are metal and plastic. However, we further prepare a plastic container to place the soil or other ground material samples to evaluate the performance of the radar system when the IED/calibration target is buried with ground samples. The difference of ground samples can make changes to the imaging results.

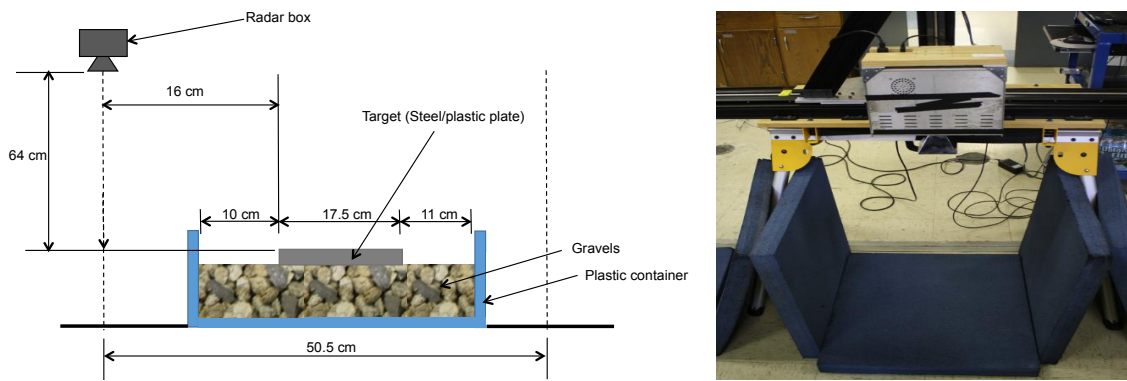


Figure 4. Laboratory Calibration System

Figure 5(b) shows a metal target which is placed on the top of the ground samples and its SAR imaging is presented in Figure 5(c). The scanning result is original and it is not reconstructed to match the metal target shape that is not presented in this paper. The purpose is to show how well the target location can be determined with real-time processing. Figure 6(b) and (c) show that the target is buried at 7.5 cm and 15 cm. The 15-cm result shows multiple scatterings from the target and it can be corrected by further developing imaging algorithms.

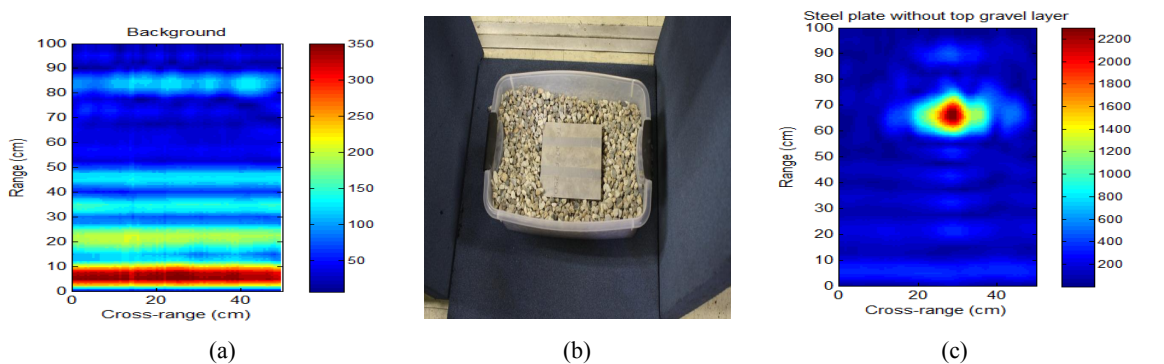


Figure 5. (a) Background without the target; (b) Metal target on ground sample; (c) SAR imaging of the scanning area.

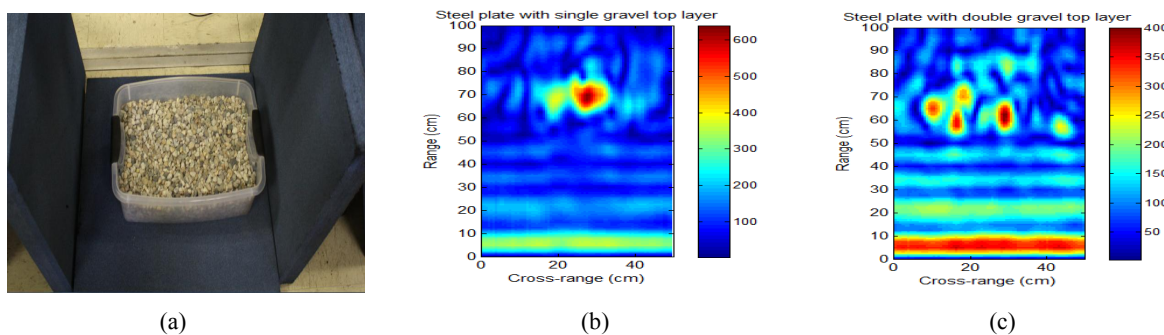


Figure 6. (a) The target buried with ground sample; (b) SAR imaging when the target is buried at 7.5-cm depth; (c) SAR imaging when the target is buried at 15-cm depth area.

2.3 Radar system

The RUIED prototype system is different than the Lab measurement. The goal of the final deliverable design is a light weight system less than 3 lb. The expensive network analyzer will be replaced by a highly integrated system, which has a fixed frequency and bandwidth based on the imaging results from the lab measurement system. Since the light weight and power consumption is always the key factors, our system can run 90 minutes with current power configuration, that can will be more mature and advanced software control functions will be developed. The final system specification is list in Table 1. The maximum detection range is varied and dependent on the transmit power of the transceiver and resolution requirements. For the radar simulation efforts, we choose parameters from the commercial available devices.

Table 1. Design parameters of the RUIED detection system.

Range	1 m to 3 m
Range Resolution	Better than 10 cm
Angular Resolution	~10 degree
Weight	3 lbs
Data Update Rate	Real-time
Antenna Gain	15 dBi
Frequency	Wideband (X-/S-/UHF-band)
Transmit Peak Power	FCC regulation
Receiver Noise Figure	4 dB

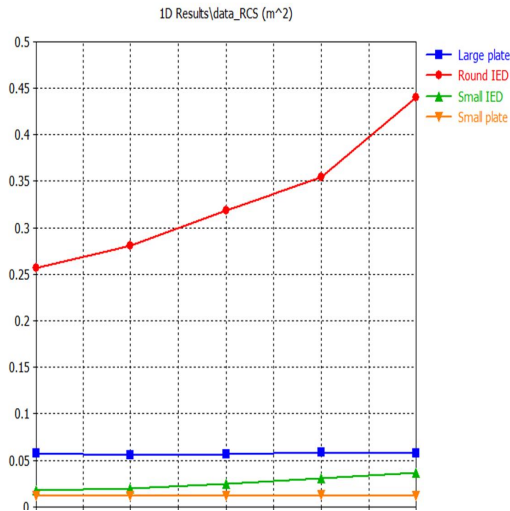


Figure 7. Simulated total RCS of four reference IEDs: Round IED: $\pi \times 19^2 \times 6 \text{ cm}^3$; (b) Small IED: $7.5 \times 7.5 \times 15.5 \text{ cm}^3$; (c) Large steel plate marker: $16 \times 17.5 \times 3 \text{ cm}^3$; (d) Small metal marker: $12 \times 4 \times 3 \text{ cm}^3$.

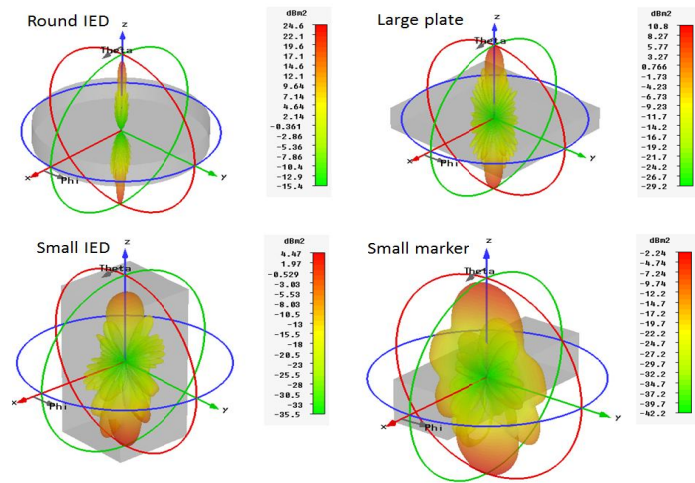


Figure 8. Simulated RCS of Round IED, Small IED, Large steel plate, and Small metal marker.

3. RCS ANALYSIS OF IED AND SAR IMAGING SIMULATION

RCS characteristic of the detecting IEDs is one of the major performance parameters of the radar system. The RCS information assists to process the radar imaging which affects the hardware requirement and radar resolution. We have selected four objects as the reference of IEDs, which include: (a) Round IED, (b) Small IED, (c) Large steel plate marker, and (d) Small metal marker. The total RCS, which is defined as the ratio of the scattered power to the intensity of the incident plane wave, of these four IEDs have been simulated in wideband, as shown in Figure 7. With this broad bandwidth, it helps understand their radiation characteristics as it changes between -3 to -17 dBsm and basically increase with the frequency. It can be seen that the round IED and the large plate IED have larger RCS values. Within the X-

band, the RCS is relative stable and the variation very small to each object. Figure 8 shows the 3D RCS of these four targets. The peak RCS of these IEDs is happened along the $\pm z$ -axis, i.e., the incidence angle (θ, ϕ) at $(0, 0)$ and $(180, 0)$. The RCS values of those IEDs with and $(90, \phi)$ degrees have been obtained is minimum. Therefore, it can be expected that the incident angle of the radar antenna will present different SAR images. The RCSs at different frequencies are shown in Figure 9.

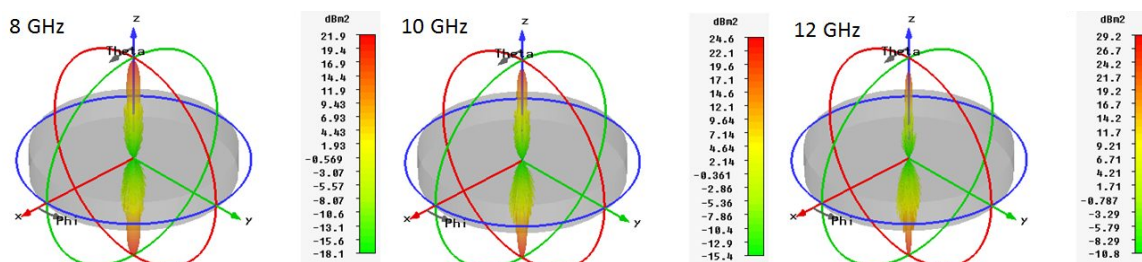


Figure 9. Simulated RCS of Round IED at different frequencies. The unit is in dBsm.

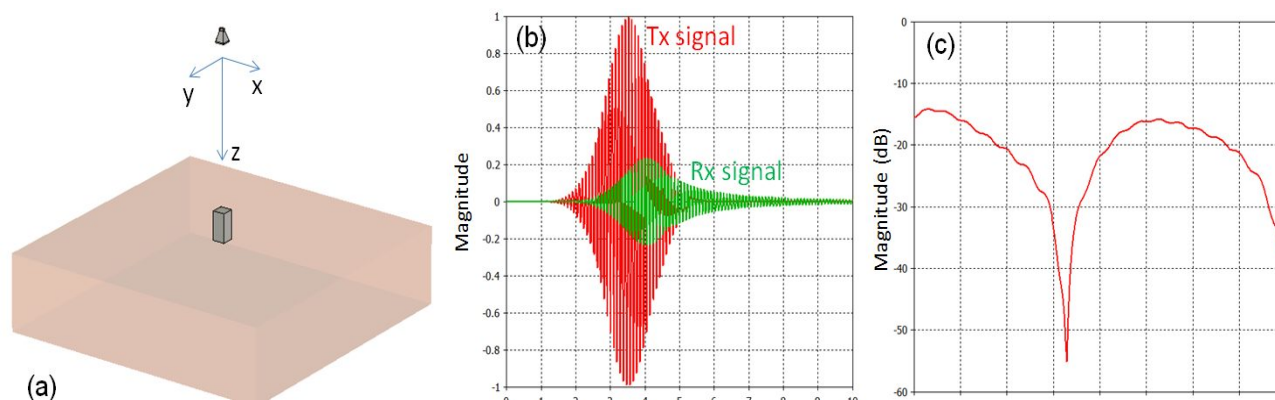


Figure 10. (a) Environment to emulate the SAR analysis where the environment medium is “dry sandy soil” ($\epsilon_r = 3.2$, $\mu_r = 1.0$, $\sigma = 0$); (b) Simulated Gaussian waveform of the transmit/receive signal; (c) the return loss of the horn antenna.

4. SIMULATION OF FIELD SCANNING TO DETECT IED

The goal of this RUIED system design is to inspect the location of the IED through the CW radar SAR imaging. The RCS is one of important radar parameters, which especially impacts the transmitting power, amplifier, and the antenna system. The SAR imaging will be the final results to be presented. To verify the concept of our system, it’s able to use a 3-D electromagnetic simulator to emulate the transmitting and reflected signals which will be used as the input raw data for the signal processing.

The simulation environment is shown in Figure 10(a) where the frequency range is 8-1 ($\Delta f = 20$ MHz) and the sampling number is 201 points. The short pulse signal and Gaussian signal are two good choices to start with, as the input signal of the SAR imaging. Figure 10(b) shows an example of the input/output Gaussian signals through the horn antenna whose return loss is shown in Figure 10(c). The horn antenna is a linear polarized antenna. The waveform (period) is decided by the bandwidth and the sampling points, in which the magnitude is normalized to one.

To know how the electromagnetic characteristic changes, we consider the placement of the IED and the incidence angle at 0 and 45 degrees. We use the small IED presented previously here and the set the frequency is at certain frequency. The initial distance from the antenna to the IED is 100 cm. All cases use the same boundary condition. The electromagnetic field distribution on XZ and XY planes at $\theta = 0^\circ$ are illustrated in Figures 18-19, and that at $\theta = 45^\circ$ are

shown in Figures 13-14, respectively. The information useful for the radar signal processing is the echo signals from the IED. Depending on the IED location relative to the soil, it gives different time-domain characteristics (reflection echo), which can be used for the SAR imaging. Figure 11(a) and Figure 11(b) shows similar features before the IED is totally buried into the soil. When the IED is buried into the soil, as shown in Figure 11(c) and Figure 11(d), the echo signals become more completed, especially inside the soil. Similar trend can be observed in Figure 12. Figures 13-14 show different wave behaviors when the incidence angle is 45 degree.

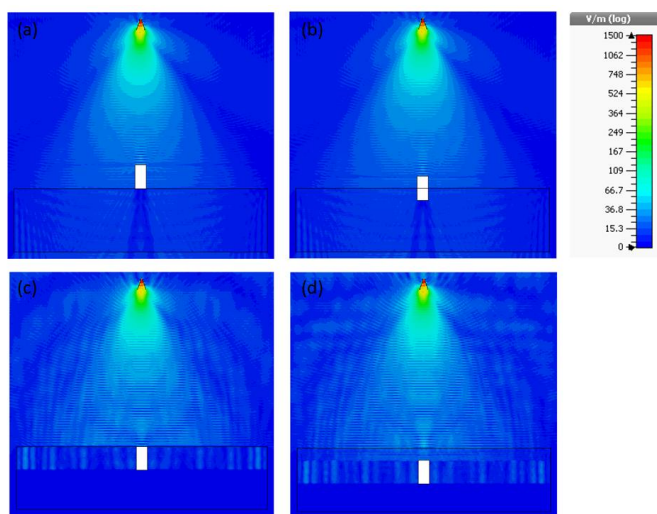


Figure 11. Simulated E-field distributions at $\theta = 0^\circ$ when the small IED is (a) on the soil, (b) 50% buried, (c) one side exposed, and (d) 100% buried.

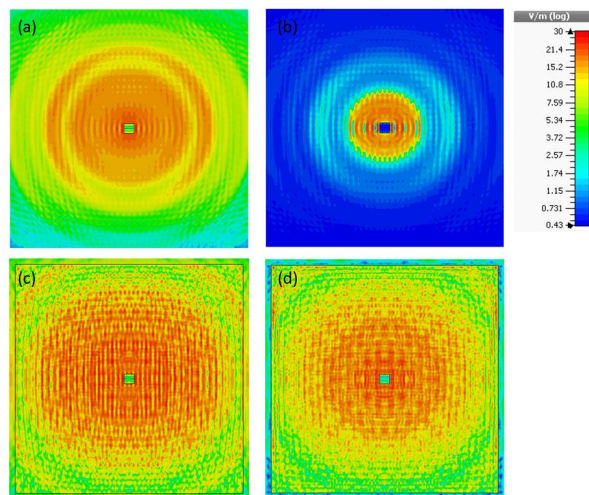


Figure 12. Simulated E-field distributions at $\theta = 0^\circ$ when the small IED is (a) on the soil, (b) 50% buried, (c) one side exposed, and (d) 100% buried, where the cut-plane is on the top side of the IED.

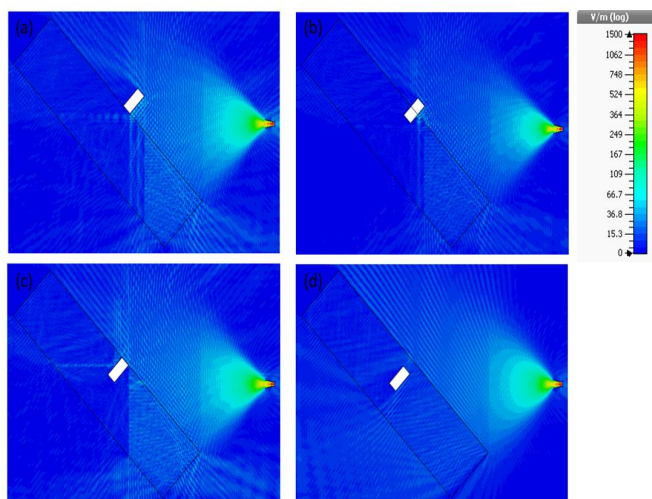


Figure 13. Simulated E-field distributions at $\theta = 45^\circ$ when the small IED is (a) on the soil, (b) 50% buried, (c) one side exposed, and (d) 100% buried.

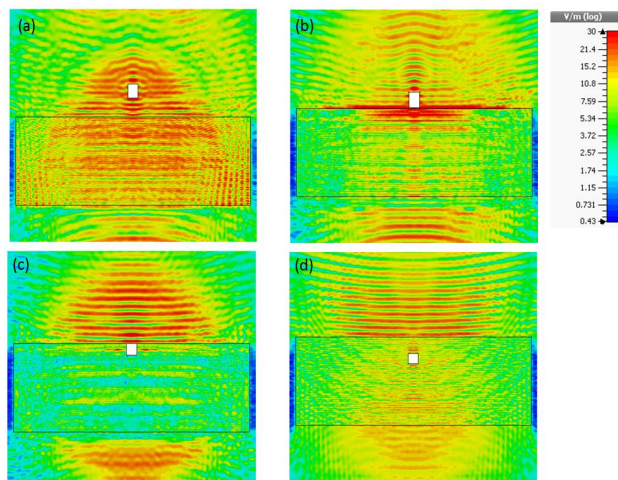


Figure 14. Simulated E-field distributions at $\theta = 45^\circ$ when the small IED is (a) on the soil, (b) 50% buried, (c) one side exposed, and (d) 100% buried, where the cut-plane is on the top side of the IED.

5. SYSTEM SETUP FOR FIELD SCANNING

To demonstrate the field applicability of the proposed RUIED prototype, a sand field has been selected in the field test and shown schematically in Figure 15(a). A custom-built cart is used to carry the RUIED prototype to simulate the airborne radar of subsurface IED targets, as shown in Figure 15(b). A small marker (4 cm by 12 cm) and a large marker

(16 cm by 17.5 cm) are placed on the surface of the sand field, while one small IED target (7.5×7.5×15.5 cm³) and one large round IED target (19 cm diameter, 6 cm height) are buried in the subsurface at a depth of 3 cm. All markers and simulated IED targets are made of PEC. Pictures of the markers and IED targets are given in Figure 16. In the field test, two incident angles are chosen, which are 0 degree (normal incidence) and 10 degree (oblique incidence). Figure 17 shows the RUIED prototype in the sand field. In both incidence schemes, the background radar image is collected with the markers only. HH and VV polarizations are applied in the field test.

In the normal incidence of HH polarization, scanned radar images of the sand field background with and without two IED targets are illustrated in Figure 18. In Figure 18(b), the locations of both small and large IED targets in the subsurface are detected by enhanced return signals. VV polarized radar images are collected and shown in Figure 19. In both Figures 18(b) and 19(b), the locations of IED targets are indicated by white dashed lines. The oblique incidence results are shown in Figures 20 and 21.

The effect of incident angle can be observed by comparing Figure 18 with Figure 20 (HH polarization), and Figure 19 with Figure 21 (VV polarization). For the two simulated IED targets considered in this testing case, the normal (perpendicular) incidence provides a better detectability. Regarding to the polarization, it seems there is no much impact of polarizations on the detectability of subsurface IED targets with SAR images.

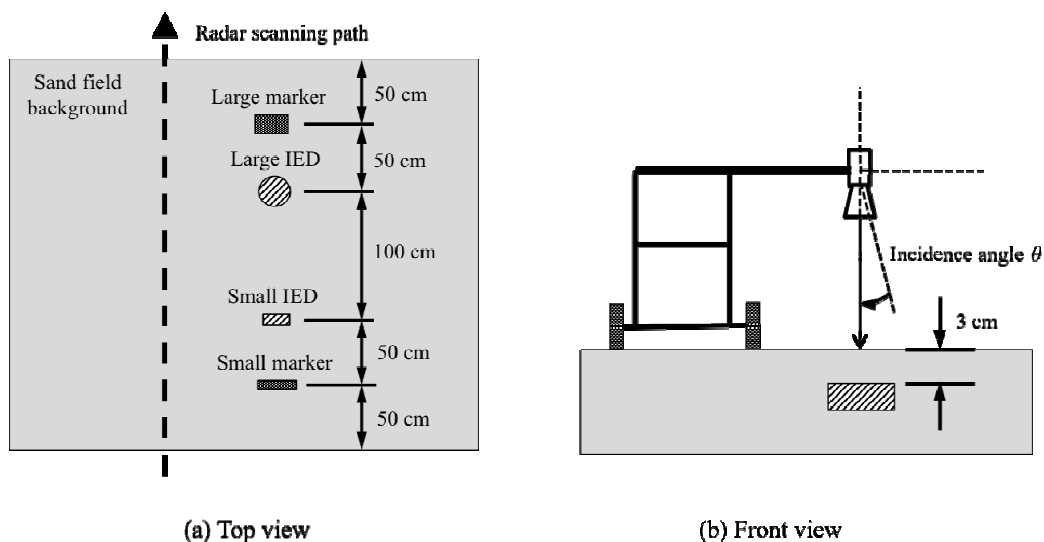


Figure 15. (a) Top view and (b) front view of the sand field.



(a) Small marker



(b) Large marker



(c) IED target

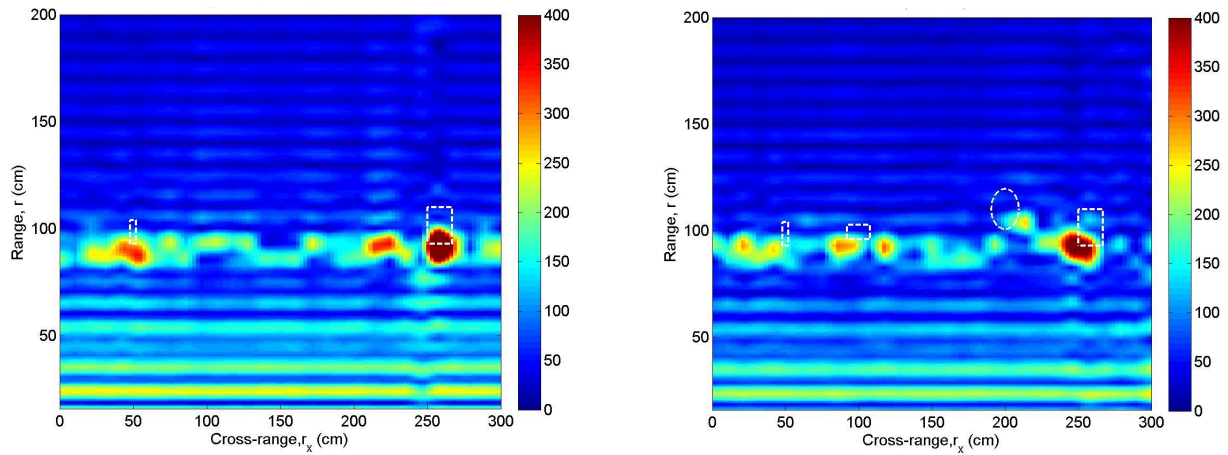


(d) Large round IED

Figure 16. Markers and simulated IED targets used in the field test.



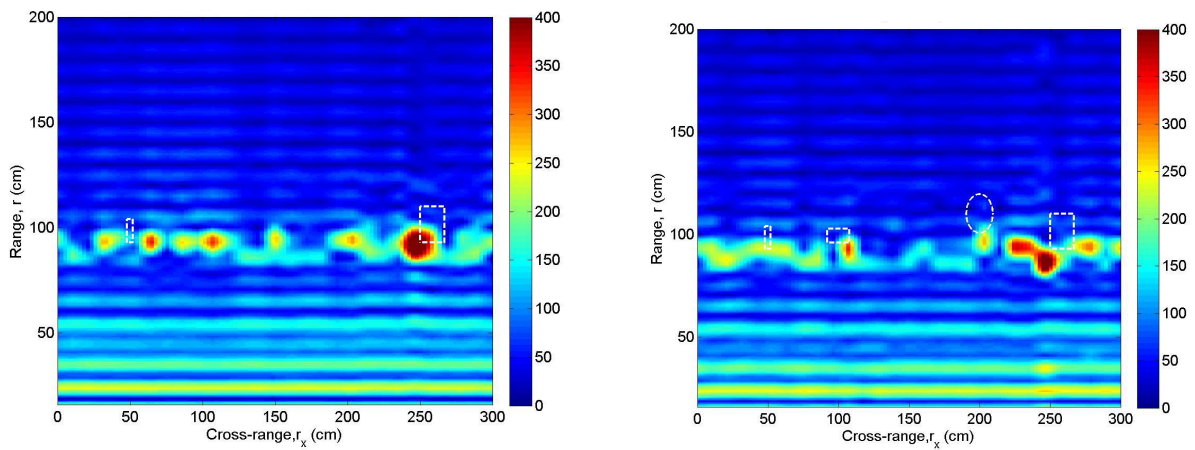
Figure 17. Airborne field test of the RUIED in a sand field.



(a) Background without IED targets

(b) With IED targets

Figure 18. Radar images generated by the RUIED prototype at 0 degree, HH polarization.



(a) Background without IED targets

(b) With IED targets

Figure 19. Radar images generated by the RUIED prototype at 0 degree, VV polarization.

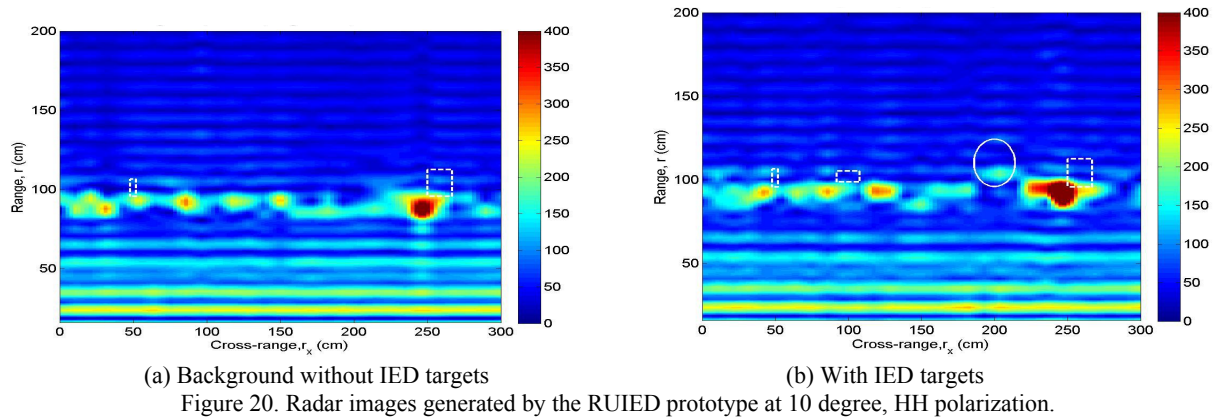


Figure 20. Radar images generated by the RUIED prototype at 10 degree, HH polarization.

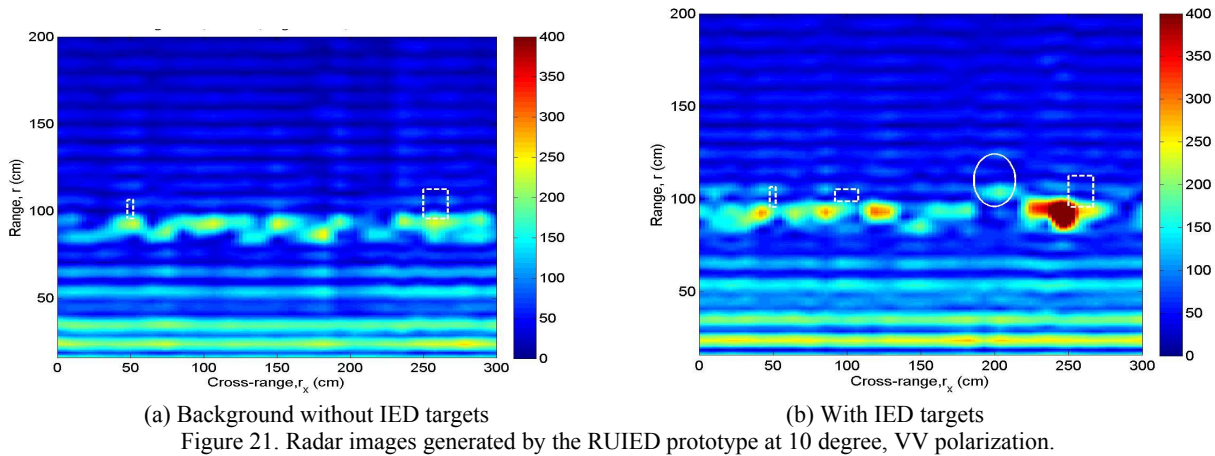


Figure 21. Radar images generated by the RUIED prototype at 10 degree, VV polarization.

6. FUTURE WORKS AND CONCLUSIONS

In this work, we have finished the radar system design which has been integrated with a rotary drone and a ground control station. A laboratory environment and a field measurement system for concept verification, calibration, data collection, and RCS/SAR imaging have been completed. The numerical simulation model, which can predict the reflection and scattering of targeted IED signals, will be developed to understand the theoretical properties of the IEDs that can generate the associated RCSs for different ground types as well as buried depths. Three dimensional SAR images will be obtained with the preprogrammed UAV flight path planning. The full-scale prototype RUIED system is shown in Figure 22. Several flight tests in the fields have been performed with certified FAA pilots and the research results will be presented in future publications and conferences.



(a) RUIED system on the ground



(b) RUIED system in a flight test

Figure 22. RUIED system under operation

REFERENCES

- [1] Yu, T.-Y., “Distant damage assessment method for multi-layer composite systems using electromagnetic waves”, *Journal of Engineering Mechanics*, ASCE, 137 (8): 547-560 (2011).
- [2] Su, Che-Fu., Tzu-Yang Yu, C.-P. Lai and Y.-J. Ren, “Wideband Subsurface Radar for Bridge Health Monitoring and Nondestructive Evaluation,” *SPIE 2013 Smart structures/NDE, March 10-14, (2013)*.
- [3] Lai, C.-P., and R. M. Narayanan, “Through Wall Surveillance Using Ultrawideband Random Noise Radar: Theory, Design Considerations, and Data Analysis”, *Aerospace and Electronic Systems*, IEEE Trans., Vol. 46, October (2010).
- [4] Skolnik, M. I., [Radar Handbook], Second Edition, McGraw-Hill, Boston & New York, Chap.21 (1990).
- [5] Oppenheim, A. V., Willsky, A. S., and Nawab, S. H., [Signals & Systems], Second Edition, Prentice Hall, Upper Saddle River, New Jersey, (1996).